On the sound produced by flow interaction with a wall mounted finite length cylinder

Danielle J. Moreau and Con J. Doolan

School of Mechanical Engineering, The University of Adelaide, Adelaide, South Australia, 5005, Australia

ABSTRACT

A cylinder immersed in flow is often considered a source of unwanted sound and is relevant to a wide range of engineering applications including aircraft landing gear, rail pantographs and automotive side-mirrors. To investigate this flow-induced noise source, this paper examines the sound generated by a wall mounted finite length circular cylinder in cross-flow. Noise measurements have been taken in an anechoic wind tunnel at the University of Adelaide at a range of flow speeds and for a variety of aspect ratios (cylinder length to diameter ratio) to determine the influence of these parameters on noise generation. The experimental data presented in this paper give further insight into the underlying sound generation mechanism and can be used to validate numerical predictions of flow-induced noise from wall mounted finite length cylinders.

1 INTRODUCTION

With the growing need for air, road and rail travel, more people are being exposed to transport noise and it is increasingly being considered an important public health issue. Aerodynamic sound is a major constituent of the noise produced by modern transport vehicles and the sound generated by cylindrical objects in cross-flow is an important source of this flow-induced noise. For example, cylindrical objects are found in aircraft landing gear, rail pantographs and automobile appendages. In fact, cylindrical geometries are present in a broad range of engineering applications such as stacks or cooling towers, bridge piers, chimneys, masts, cables and wires. As the noise produced by flow interaction with a cylinder is relevant to a wide range of applications, it is important that the governing noise generation mechanism is well understood and that methods are developed so engineers can accurately predict the noise radiated into the far-field.

The great majority of studies on the noise produced by flow interaction with a cylindrical object have focused on Aeolian tone generation from a two-dimensional circular cylinder (of effectively infinite length) in uniform cross-flow (Curle, 1955, Gerrard, 1955, Phillips, 1956, Schlinker et al., 1976, Cox et al., 1998, Inoue and Hatakeyam, 2002, Fujita et al., 2006, Cheong et al., 2008). Very little research has been conducted on the sound generated by flow over a wall mounted finite length cylinder. Experimental data sets on this topic are rare despite their importance for understanding the physical noise generation mechanisms responsible for flow-induced cylinder noise.

The flow field around a wall mounted finite length cylinder is complex, three-dimensional and consists of a number of interacting vortex systems. In addition to the alternating spanwise vortex shedding (Kármán vortex street) observed for a two-dimensional cylinder, end effects are also present. Vortex structures form due to flow over the cylinder tip and at the junction of the cylinder and the wall. The vortex systems can merge and interact to produce a highly complex wake (Palau-Salvador et al., 2010). For a wall mounted finite length cylinder, the flow field structure and the radiated sound will depend on Reynolds number, aspect ratio (the

ratio between cylinder length and diameter) and the ratio between the cylinder length and the wall boundary layer thickness (Becker et al., 2008).

King and Pfizenmaier (2009) are one of the very few to experimentally investigate flow-induced noise from finite length cylinders. Their study presents noise measurements for cylinders of various cross-section (circular, elliptical and square) and aspect ratio (L/D = 2 - 35) in a free jet at Reynolds numbers of $Re_D > 4.2 \times 10^4$, based on cylinder diameter. Aspect ratio was found to be an important parameter in determining the peak frequency and sound level of the radiated noise. In addition, cylinders with an elliptical cross-section were identified as producing the lowest overall noise levels.

This paper presents results of an experimental study on the noise produced by flow interaction with a wall mounted finite length circular cylinder. Far-field noise measurements have been taken in an anechoic wind tunnel at a range of Reynolds numbers ($Re_D = 1 \times 10^4 - 1.4 \times 10^4$) and cylinder aspect ratios (L/D = 1.6 – 22.6). This paper aims to provide benchmark acoustic data for a wall mounted finite length circular cylinder in cross-flow and to provide further insight into the fundamental physics of the flow-induced noise generation mechanism. It is worth noting that the results presented in this paper are the preliminary results of a much larger study examining this type of noise source.

2 EXPERIMENTAL METHOD

2.1 Anechoic wind tunnel facility

Testing was conducted in the anechoic wind tunnel at the University of Adelaide. The anechoic wind tunnel test chamber is 1.4 m × 1.4 m × 1.6 m (internal working volume) and has walls that are acoustically treated with foam wedges to provide a reflection free environment (ideally) above 250 Hz. The facility contains a rectangular contraction with a height of 75 mm and a width of 275 mm. The maximum flow velocity of the free jet is ~40 m/s and the free-stream turbulence intensity is low at 0.33%.

2.2 Test models

Fourteen cylinders with circular cross-section are used in this study. Each cylinder was fixed (one at a time) to a side plate which was in turn flush mounted to the contraction flange so that the cylinder length axis was perpendicular to the direction of the flow, as shown in Fig. 1. The aluminium side plate has a length of 300 mm in the streamwise direction and a width of 155 mm in the vertical direction. As shown in Fig. 1, the centre of the cylinder is positioned 30 mm downstream of the jet exit plane at the vertical centreline of the jet.

The fourteen cylinders have the same diameter, D, equal to 6 mm and a different length, L, between δ and 14δ, where δ is the boundary layer thickness on the side plate at the cylinder location at $U_\infty = 35$ m/s. The side plate boundary layer thickness, δ, at the cylinder location was measured prior to the cylinder being attached to the side plate and was found to be 9.7 mm (see Section 3.1). The cylinders therefore have a length (or span) between $L = 9.7$ and 135.8 mm and an aspect ratio between $L/D = 1.6$ and 22.6.

2.3 Measurement equipment and procedure

Hot-wire anemometry was first used to measure properties of the side plate boundary layer at the cylinder location, prior to the cylinder being attached to the side plate. A TSI 1210-T1.5 single wire probe with wire length of 1.27 mm and a wire diameter of 3.81 μm was used in experiments. The sensor was connected to a TSI IFA 300 constant temperature anemometer system and positioned using a Dantec automatic

traverse with 6.25 μm positional accuracy. The traverse allowed continuous movement in the streamwise (x), spanwise (y) and vertical (z) directions. The co-ordinate system used in this study is shown in Fig. 1. Velocity measurements were recorded at a flow speed of $U_\infty = 35$ m/s. At each measurement location, velocity data were recorded using a National Instruments board at a sampling frequency of 50 kHz for a sample time of 4 s.

Acoustic measurements were recorded with each of the fourteen cylinders mounted to the side plate. Noise data were measured at a single observer location using a B&K ½" microphone (Model No. 4190) located 515 mm directly above the centre of the longest cylinder with $L = 14\delta$ (aspect ratio $L/D = 22.6$). To provide isolation from wind noise, a wind sock was placed on the microphone prior to data collection. Acoustic measurements were recorded at three flow speeds between $U_\infty = 25$ and 35 m/s, corresponding to Reynolds numbers of $Re_D = 1 \times 10^4 - 1.4 \times 10^4$, based on cylinder diameter. At each selected flow speed, noise data were recorded using a National Instruments board at a sampling frequency of 50 kHz for a sample time of 8 s.
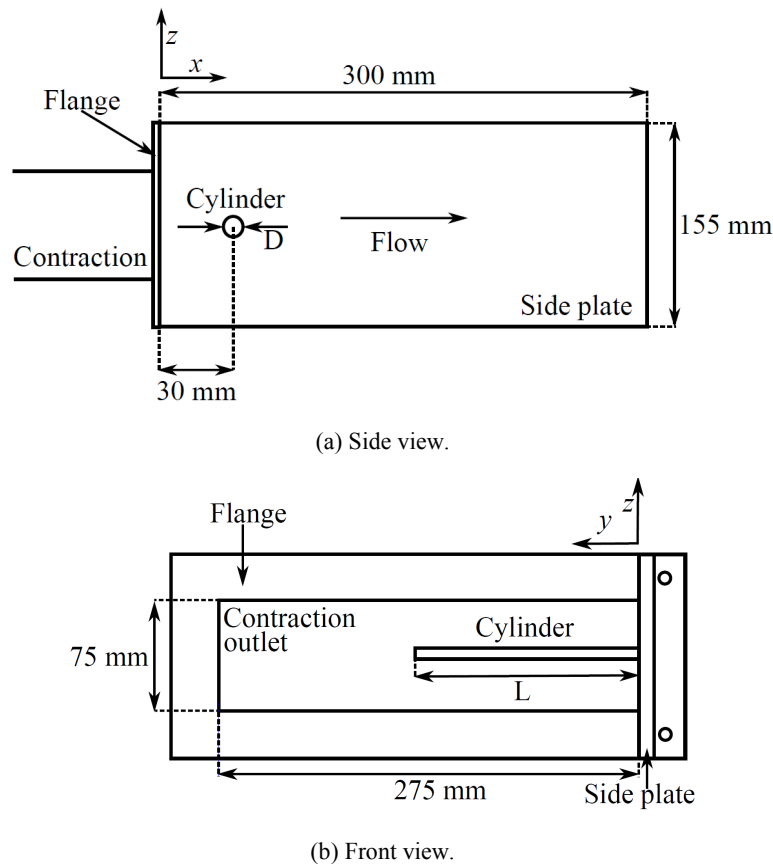

(a) Side view.

(b) Front view.

Figure 1. Schematic diagram of the cylinder in the anechoic wind tunnel test section.

3 EXPERIMENTAL RESULTS AND DISCUSSION

3.1 Side plate boundary layer characteristics

Properties of the side plate boundary layer at the cylinder location are presented in this section. These measurements were taken prior to the cylinder being attached to the side plate and provide information on the state of the boundary layer at the cylinder location.

The side plate boundary layer mean velocity profile ($\overline{U}/U_\infty$) at the cylinder location at $U_\infty = 35$ m/s is shown in Fig. 2(a). In this figure, the mean velocity profile is compared with the $1/7^{th}$ power law for a turbulent boundary layer and the Blasius boundary layer solution for laminar flow (Cebeci and Bradshaw, 1977). Figure 2(a) shows that the side plate boundary layer approximates the $1/7^{th}$ power law profile indicating that the flow is well-developed and in a turbulent state on the side plate at the cylinder location. At this measurement location, the boundary layer thickness, calculated as the distance from the side plate to the point where the flow velocity has reached 99% of the free-stream velocity, is $\delta = 9.7$ mm.

Figure 2(b) shows the normalised rms velocity fluctuations ($\overline{u}'/U_\infty$) in the boundary layer at the cylinder location at $U_\infty = 35$ m/s. This figure shows that the turbulent energy is at a maximum in the inner boundary layer region at $y = 1.5$ mm above the plate surface. After this point, there is a reduction in the turbulent energy in the outer boundary layer and in the free-stream.

### 3.2 Cylinder acoustic spectra

Figure 3 shows 2D spectral plots of the noise produced by the cylinders at $U_\infty = 25$ - 35 m/s. For closer inspection, Fig. 4 shows single line acoustic spectra for cylinders with four selected aspect ratios of $L/D = 1.6$, 3.2, 12.9 and 22.6 at $U_\infty = 25$ - 35 m/s.

At the highest aspect ratio of $L/D = 22.6$, Figs. 3 and 4(a) show that a high amplitude double peak is observed in the cylinder noise spectra at flow speeds between $U_\infty = 25$ and 35 m/s. This double peak (referred to as the dominant double peak hereafter) remains visible in the noise spectra for cylinders with an aspect ratio down to $L/D = 19.4$. The frequency and magnitude of the dominant double peak is observed to reduce with aspect ratio and flow speed (see Figs. 3 and 4(a)).

The dominant double peak observed in the noise spectra for cylinders with an aspect ratio between $L/D = 19.4$ and 22.6 is accompanied by a low amplitude, low frequency single peak (e.g. at 394 Hz for $U_\infty = 35$ m/s in Figs. 3(a) and 4(a)). The frequency of this single peak (referred to as the secondary single peak hereafter) remains constant for a reduction in aspect ratio but is reduced with flow speed.

The three peaks (those of the dominant double peak and secondary single peak) observed in the noise spectra for cylinders with an aspect ratio between $L/D = 19.4$ and 22.6 are likely due to three vortex systems. It is speculated that unsteady tip vortices form due to downwash over the cylinder tip and alternating Kármán-type vortex shedding occurs along part of the cylinder span. Additionally, vortex structures are produced at the cylinder-wall junction. For an aspect ratio of between $L/D = 19.4$ and 22.6, the cylinder is long

enough to have a region that is free of end effects so that alternating Kármán-type vortex shedding may occur undisturbed behind a large part of the cylinder. The strength of this vortex shedding will reduce as aspect ratio is also reduced because the flow from the cylinder end will disturb a greater proportion of the span as the cylinder length is reduced.
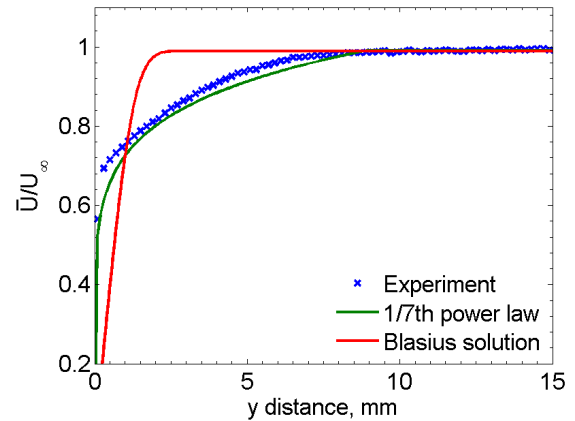
(a) Normalised boundary layer mean velocity profile at $U_\infty = 35$ m/s compared to the $1/7^{th}$ power law profile and the Blasius solution.
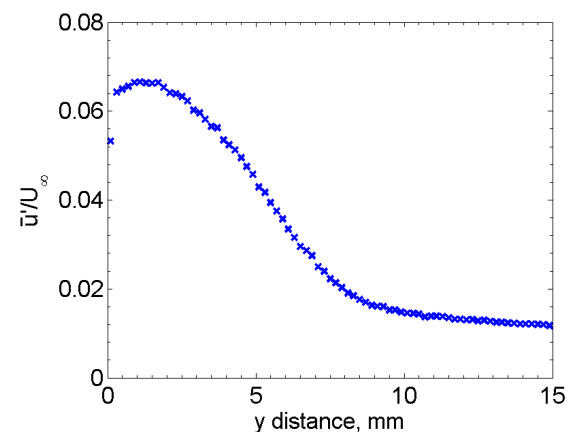
(b) Normalised rms velocity fluctuations in the boundary layer at $U_\infty = 35$ m/s.

Figure 2. Side plate boundary layer mean velocity and rms profiles at the cylinder location for $U_\infty = 35$ m/s.

When the aspect ratio is reduced to $L/D = 17.8$, the dominant double peak observed for cylinders with an aspect ratio of $L/D > 19.4$ becomes a single peak in the noise spectra at flow speeds between $U_\infty = 25$ and 35 m/s. This single peak (referred to as the dominant single peak hereafter) is observed for cylinders with an aspect ratio between $L/D = 9.7$ and 17.8 (see Figs. 3 and 4 (b)). Additionally, the secondary single peak that does not change in frequency with the aspect ratio is also visible in these noise spectra.

The two single peaks observed in the noise spectra for cylinders with an aspect ratio of between $L/D = 9.7$ and 17.8 are likely due to tip vortex structures associated with downwash over the cylinder tip and vortex structures produced at the cylinder-wall junction. It is speculated that in this case, cylinder end-effects have an influence over the entire cylinder span.

No peaks are observed in the noise spectra for cylinders with an aspect ratio between $L/D = 4.9$ and 8.1 at flow speeds

between U_∞ = 25 and 35 m/s (see Fig. 3). This indicates that vortex shedding is suppressed for cylinders with an aspect ratio between L/D = 4.9 and 8.1 preventing acoustic tone generation.

Interestingly, a dominant single peak reappears in the noise spectra when the cylinder aspect ratio is reduced to L/D = 3.2 at flow speeds between U_∞ = 25 and 35 m/s (see Fig. 3 and 4(c)). The magnitude of the peak is low indicating that the vortex shedding process responsible for this peak is weak.

When the cylinder aspect ratio is further reduced to L/D = 1.6, no peaks are again observed in the noise spectra at flow speeds between U_∞ = 25 and 35 m/s (see Fig. 3 and 4(d)). Figure 4(d) shows that only broadband noise is measured in this case.

Table 1 provides a summary of the peaks observed in the noise spectra for cylinders with an aspect ratio between L/D = 1.6 and 22.6 at flow speeds between U_∞ = 25 and 35 m/s. It is clear that the radiated sound field is produced by a very complex flow structure and that the flow field around the wall mounted finite length cylinder must be examined in conjunction with the sound field to gain a better understanding of the noise generation mechanism.

Table 1. Peaks observed in the noise spectra for cylinders with aspect ratio between L/D = 1.6 and 22.6 at flow speeds of U_∞ = 25 - 35 m/s.

L/D	Dominant double peak (P1)	Dominant single peak (P2)	Secondary single peak (P3)	No peak
22.6	x		x	
21.0	x		x	
19.4	x		x	
17.8		x	x	
16.2		x	x	
14.6		x	x	
12.9		x	x	
11.3		x	x	
9.7		x	x	
8.1				x
6.5				x
4.9				x
3.2		x		
1.6				x

(a) U_∞ = 35 m/s.
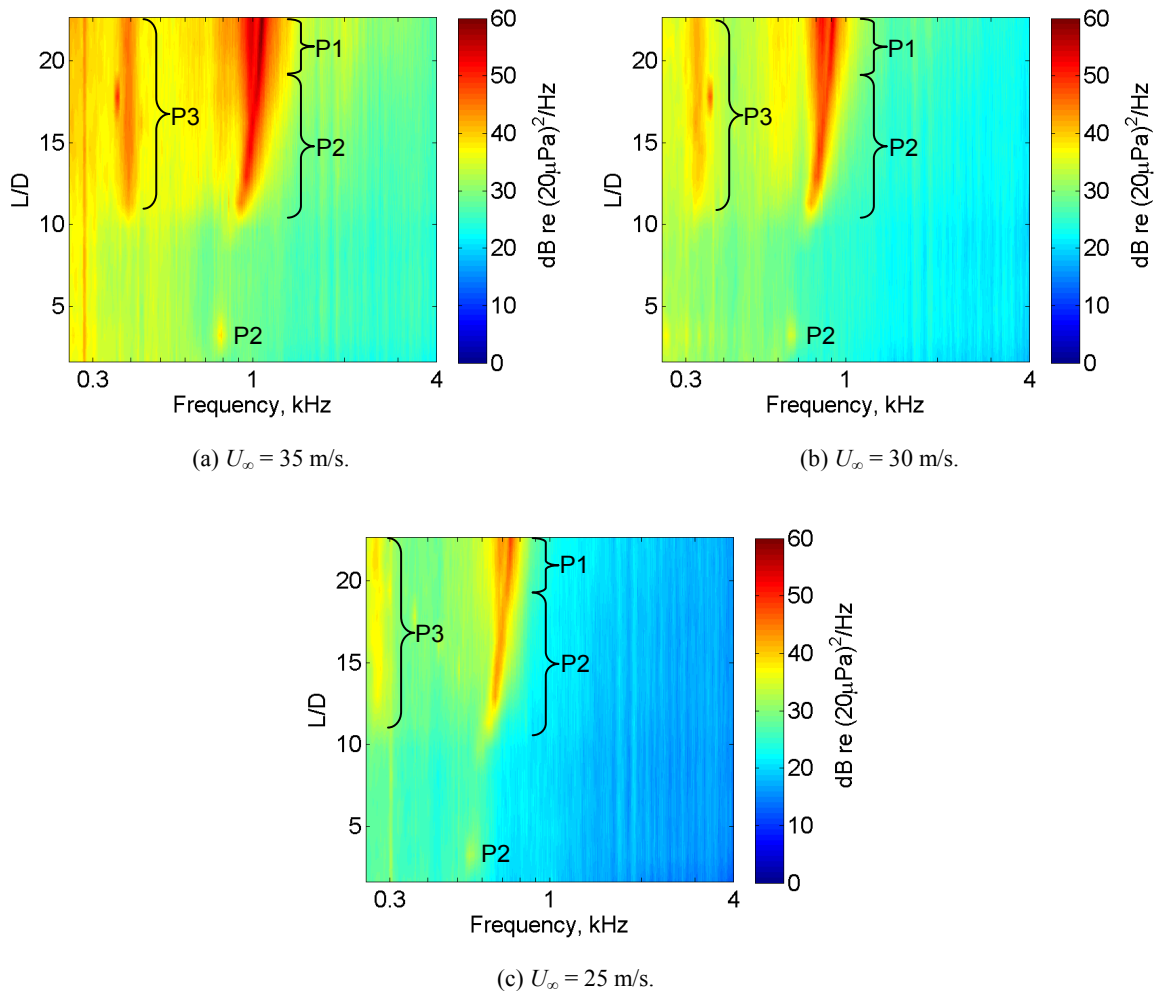

(b) U_∞ = 30 m/s.

(c) U_∞ = 25 m/s.

Figure 3. Far-field acoustic spectral maps for the circular cylinder at U_∞ = 25 – 35 m/s. P1 refers to a dominant double peak, P2 refers to a dominant single peak and P3 refers to a secondary single peak.

(a) $L/D = 22.6$.

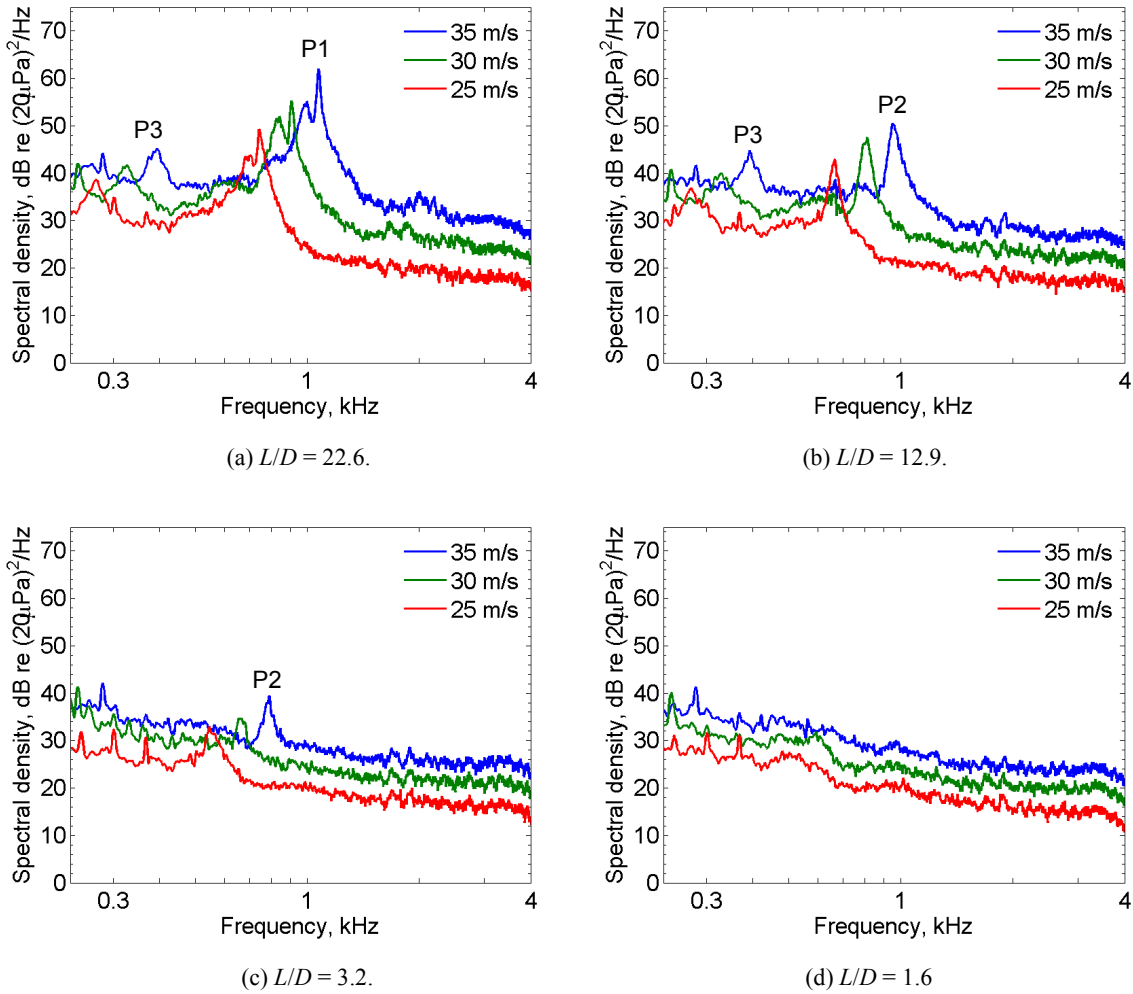(b) $L/D = 12.9$.

(c) $L/D = 3.2$.

(d) $L/D = 1.6$

Figure 4. Far-field acoustic spectra for the circular cylinder at $U_\infty = 25 - 35$ m/s. P1 refers to a dominant double peak, P2 refers to a dominant single peak and P3 refers to a secondary single peak.

In their study on the noise produced by a finite length cylinder in cross-flow, King and Pfizenmaier (2009) did not observe acoustic tones for a cylinder aspect ratio of $L/D = 10$ and $L/D < 3$. In addition, a double peak was observed in their noise spectra for a cylinder aspect ratio of $L/D > 30$. While containing some notable similarities, the results of King and Pfizenmaier (2009) do not agree with the acoustic measurements in this study. These discrepancies are most likely due to differences in Reynolds number and experimental setup as King and Pfizenmaier (2009) conducted their experiments in a free jet and not in a turbulent boundary layer.

3.3 Overall sound pressure level

Figure 5 shows the variation in overall sound pressure level with cylinder aspect ratio at flow speeds between $U_\infty = 25$ and 35 m/s. This figure shows that there is a clear increase in overall sound pressure level with flow speed. The noise level reduces significantly with cylinder aspect ratio when either a dominant double or single peak is observed in the noise spectra. Conversely, the overall sound pressure level remains fairly constant for cylinders that do not produce an acoustic tone.
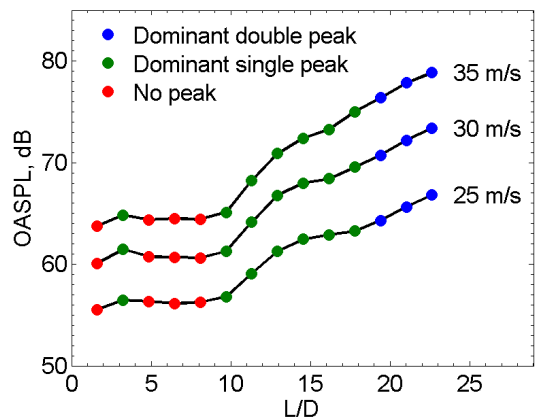

Figure 5. Overall sound pressure level variation with L/D for the circular cylinder at $U_\infty = 25 - 35$ m/s.

3.4 Acoustic scaling

According to Curle (1955), the noise radiation characteristic of a cylinder is dipole like. The dipole sound is related to the unsteady forces created by fluid flow on the cylinder surface. Therefore, cylinder noise is expected to scale with M^6 where M is the free-stream Mach number. The spectra for cylinders with 3 selected aspect ratios of L/D = 1.6, 12.9 and 22.6 at U_∞ = 25 - 35 m/s are normalised by M^6 in Fig. 6 according to:

$$\text{Scaled spectra} = \text{spectral density} - 60\log_{10}(M). \qquad (1)$$

In Fig. 6, the scaled cylinder noise is plotted against the non-dimensional Strouhal number based on cylinder diameter, D:

$$St_D = \frac{fD}{U_\infty}, \qquad (2)$$

where f is frequency. Strouhal (1878) found that the frequency of the Aeolian tone produced by a circular cylinder in cross-flow is proportional to freestream velocity, U_∞, and inversely proportional to the cylinder diameter, D.

Figure 6 shows that an M^6 power law gives a good collapse of the cylinder noise spectra at flow speeds between U_∞ = 25 and 35 m/s. Spectra that are originally spread by almost 40 dB are collapsed to within 8 dB. The cylinder noise levels therefore increase according to an M^6 power law indicating a dipole noise source.
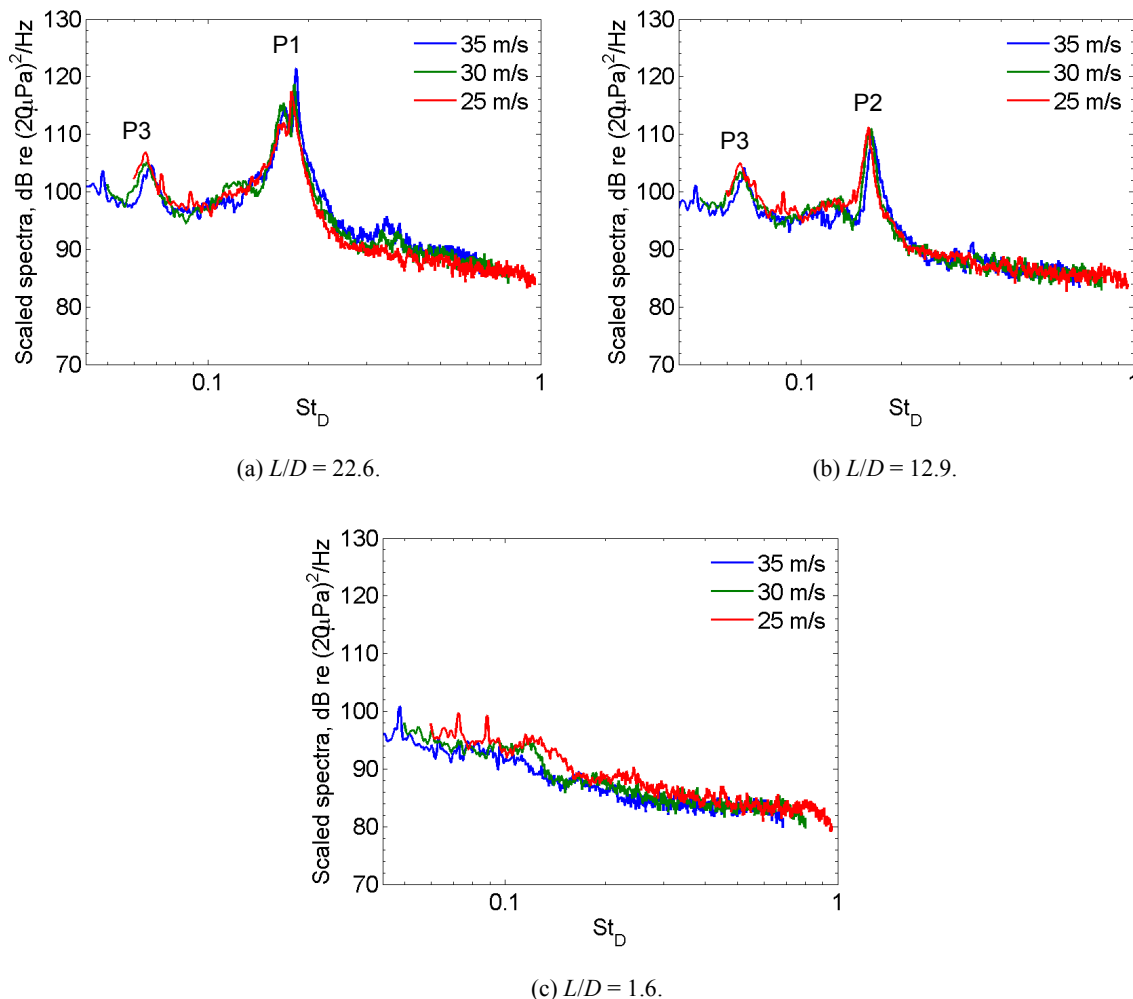
For a cylinder aspect ratio of L/D = 22.6, Fig. 6(a) shows that the dominant double peak occurs at a Strouhal number of St_D = 0.168 – 0.184. For a lower aspect ratio of L/D = 12.9, Fig. 6(b) shows that the dominant single peak occurs at a lower Strouhal number of St_D = 0.159 – 0.163. For all cylinders with aspect ratio between L/D = 9.7 and 22.6, the secondary single peak occurs at a Strouhal number of St_D = 0.065 – 0.068.

Figure 7 shows the Strouhal number, St_D, of the dominant double or single peaks as a function of cylinder aspect ratio, L/D, at flow speeds between U_∞ = 25 and 35 m/s. When a dominant double peak is produced, the two Strouhal numbers of both peaks are plotted. Figure 7 shows that for cylinders with an aspect ratio of between L/D = 1.6 and 22.6, dominant vortex shedding noise contributions occur at a Strouhal number of between 0.131 and 0.184.

Figure 7 shows that both flow speed, U_∞, and aspect ratio, L/D, have an influence on the peak Strouhal number. A reduction in Strouhal number is observed for a reduction in both flow speed and aspect ratio. Reducing the aspect ratio from L/D = 22.6 to 9.7 at U_∞ = 35 m/s reduces the peak Strouhal number from St_D = 0.184 to 0.145 (a 21% reduction).

(a) L/D = 22.6.

(b) L/D = 12.9.

(c) L/D = 1.6.

Figure 6. Scaled far-field acoustic spectra as a function of Strouhal number for the circular cylinder at U_∞ = 25 – 35 m/s. P1 refers to a dominant double peak, P2 refers to a dominant single peak and P3 refers to a secondary single peak.

The flow around a circular cylinder is generally classified into three regimes: subcritical ($Re_D = 2 \times 10^2 - 1 \times 10^5$), supercritical ($Re_D = 1 \times 10^5 - 4 \times 10^6$) and transcritical ($Re_D > 4 \times 10^6$) (Roshko, 1961). In this study, acoustic measurements have been taken for a finite length cylinder in flow at subcritical Reynolds numbers. In the subcritical range, a two-dimensional cylinder is expected to produce an Aeolian tone with a Strouhal number of $St_D \approx 0.2$ (Norberg, 2003). In Fig. 7, the dominant peak Strouhal reaches a maximum of $St_D = 0.184$ when the aspect ratio is $L/D = 22.6$. This is below the Strouhal number for a two-dimensional cylinder in the subcritical range.
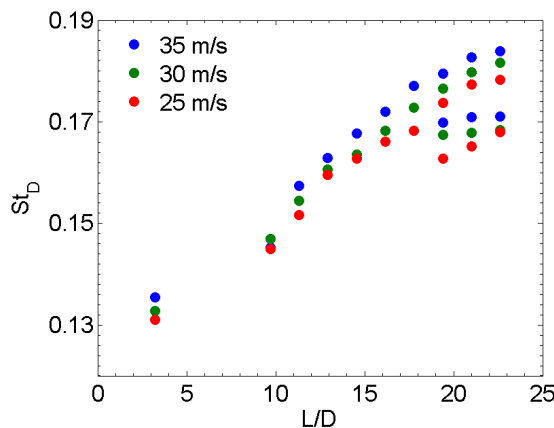

Figure 7. Dominant peak Strouhal number as a function of aspect ratio L/D for the circular cylinder at $U_\infty = 20 - 35$ m/s.

5 CONCLUSION

This paper has presented results of an experimental investigation on the noise produced by a wall mounted finite length cylinder in cross-flow. Noise measurements have been presented for a circular cylinder with aspect ratio between $L/D = 1.6$ and 22.6 at flow speeds between $U_\infty = 25$ and 35 m/s ($Re_D = 1 \times 10^4 - 1.4 \times 10^4$). Aspect ratio was found to have a significant effect on the radiated noise field. It was suggested that aspect ratio determines the number of isolated vortex shedding processes occurring from the cylinder thus explaining the different types of observed noise generation. In addition, flow speed was shown to influence the overall sound pressure level and the peak Strouhal number. As a practical guide, the results suggest that noise radiation remains low and broadband in nature when the aspect ratio is kept above 3 and below 10. The dipole scaling law of M^6 was shown to give a good collapse of the far-field noise spectra, demonstrating that the radiated sound field has dipole like radiation characteristics.

As stated earlier, the experimental investigation detailed in this paper is part of an ongoing study on the noise produced by flow interaction with a wall mounted finite length cylinder. The next stage of this study involves taking detailed measurements of the flow field in the cylinder wake with hot-wire anemometry to gain further insight into the noise generation mechanism. In addition, the flow over and noise produced by wall mounted finite length cylinders with different cross-sections (square, rectangular, elliptical etc) will also be examined.

REFERENCES

Becker, S, Hahn, C, Kaltenbacher, M and Lerch, R 2008 'Flow-induced sound of wall-mounted cylinders with different geometries', *AIAA Journal*, vol. 46, no. 9, pp. 2265 – 2281.

Cebeci, T and Bradshaw, P 1977 *Momentum Transfer in Boundary Layers,* Hemisphere Publishing Corporation, Washington.

Cheong, C, Joseph, P, Park, Y and Lee, S 2008 'Computation of Aeolian tone from a circular cylinder using source models', *Applied Acoustics*, vol. 69, no. 2, pp. 110 – 126.

Cox, J, Brentner, KS and Rumsey, CL 1998 'Computation of vortex shedding and radiated sound for a circular cylinder: subcritical to transcritical Reynolds numbers', *Theoretical and Computational Fluid Dynamics*, vol. 12, pp. 233 – 253.

Curle, N 1955 'The influence of solid boundaries upon aerodynamic sound', *Proceedings of the Royal Society of London, Series A*, vol 231, no. 1187, pp. 505 – 514.

Fujita, H, Suzuki, Y, Itou, T and Hashimoto, Y 2006 'The characteristics of the flow field around two-dimensional cylinders in relation to the Aeolian tone generation', *Proceedings of Internoise 2006*, Honolulu, Hawaii, December 3 – 6.

Gerrard, JH 1955 'Measurements of the sound from circular cylinders in an air stream', *Proceedings of the Royal Society of London, Series B*, vol. 68, pp. 453 – 461.

Inoue, O and Hatakeyam, H 2002 'Sound generation by a two-dimensional circular cylinder in a uniform flow', *Journal of Fluid Mechanics*, vol. 471, pp. 285 – 314.

King, WF and Pfizenmaier, E 2009 'An experimental study of sound generated by flows around cylinders of different cross-section', *Journal of Sound and Vibration*, vol. 328, pp. 318 – 337.

Norberg, C 2003 'Fluctuating lift on a circular cylinder: review and new measurements', *Journal of Fluids and Structures*, vol. 17, pp. 57 – 96.

Palau-Salvador, G, Stoesser, T, Frohlich, J, Kappler, M and Rodi, W 2010 'Large eddy simulations and experiments of flow around finite-height cylinders', *Flow Turbulence and Combustion*, vol. 84, pp. 239 – 275.

Phillips, OM 1956 'The intensity of Aeolian tones', *Journal of Fluid Mechanics*, vol. 1, pp. 607 – 624.

Roshko, A 1961 'Experiments on the flow past a circular cylinder at very high Reynolds number', *Journal of Fluid Mechanics*, vol. 10, no. 2, pp. 345 – 356.

Schlinker, RW, Fink, MR and Amiet RK 1976 'Vortex noise from non-rotating cylinders and airfoils', *Proceedings of the AIAA 14th Aerospace Sciences Meeting*, AIAA paper no. 76 – 81, Washington, D.C., January 26 – 28.

Strouhal V 1878 'On one particular way of tone generation', *Annual Review of Physical Chemistry*, vol. 5, pp. 216 – 251 (in German).